IP_3 receptors – lessons from analyses *ex cellula*

Ana M. Rossi and Colin W. Taylor*

Department of Pharmacology, Tennis Court Road, Cambridge, CB2 1PD, UK

*Author for correspondence: cwt1000@cam.ac.uk

Running title

IP_3 receptors

Key words

Bilayer recording; Ca^{2+} channel; Endoplasmic reticulum; Ion channel structure; IP_3 receptor; Nuclear patch-clamp; Permeabilized cell; Radioligand binding; Ryanodine receptor.

ABSTRACT

Inositol 1,4,5-trisphosphate receptors (IP_3Rs) are widely expressed intracellular channels that release Ca^{2+} from the endoplasmic reticulum (ER). We review how studies of IP_3Rs removed from their intracellular environment ('*ex cellula*'), alongside similar analyses of ryanodine receptors, have contributed to understanding IP_3R behaviour. Analyses of permeabilized cells demonstrated that the ER is the major intracellular Ca^{2+} store, and that IP_3 stimulates Ca^{2+} release from it. Radioligand binding confirmed that the 4,5-phosphates of IP_3 are essential for activating IP_3Rs, and facilitated IP_3R purification and cloning, which paved the way to structural analyses. Reconstitution of IP_3Rs into lipid bilayers and patch-clamp recording from the nuclear envelope established that IP_3Rs have a large conductance and select weakly between Ca^{2+} and other cations. Structural analyses are now revealing how IP_3 binding to the N-terminus of the tetrameric IP_3R opens the pore ~7nm away from the IP_3-binding core (IBC). Communication between the IBC and pore passes through a nexus of interleaved domains contributed by structures associated with the pore and cytosolic domains, which together contribute to a Ca^{2+}-binding site. These structural analyses provide a plausible explanation for the suggestion that IP_3 gates IP_3Rs by first stimulating Ca^{2+} binding, which leads to pore opening and Ca^{2+} release.

Introduction

Inositol 1,4,5-trisphosphate receptors (IP_3Rs) and ryanodine receptors (RyR) are the two major families of intracellular Ca^{2+}-release channels in animal cells (**Fig. 1A**). IP_3Rs are expressed in most cells, whereas RyRs have a more restricted distribution. RyRs are most abundant in excitable cells, notably in striated muscle, where they contribute to excitation-contraction coupling (**Fig. 1A**) (Van Petegem, 2014). In this review, we focus on IP_3Rs, and how methods applied to IP_3Rs removed from intact cells have contributed to our understanding of IP_3R behaviour. Progress with understanding IP_3Rs and RyRs has developed in parallel, and with this progress it became clear that the two families share structural and functional features (Baker et al., 2017; Seo et al., 2012). Hence, despite our focus on IP_3Rs, we draw also on evidence from analyses of RyRs.

Classic work by Sydney Ringer demonstrated that cardiac muscle contraction requires extracellular Ca^{2+} (Ringer, 1883). This was, with benefit of hindsight, the first of many studies to show that the contributions to physiological responses of extracellular Ca^{2+} and Ca^{2+} held within intracellular stores are entangled. For cardiac muscle, depolarization of the plasma membrane (PM) causes voltage-gated Ca^{2+} channels ($Ca_v1.2$) to open, and the local increase in cytosolic free Ca^{2+} concentration $[Ca^{2+}]_c$ is then amplified by Ca^{2+}-induced Ca^{2+} release (CICR) through type 2 ryanodine receptors (RyR2) in the sarcoplasmic reticulum (Bers, 2002) (**Fig. 1A**). CICR and the local Ca^{2+} signalling that is required to avoid CICR from becoming explosive have become recurrent themes in Ca^{2+} signalling (Rios, 2018). Fluorescent Ca^{2+} indicators and optical microscopy now allow Ca^{2+} sparks, local Ca^{2+} signals evoked by a small cluster of RyRs, to be measured with exquisite subcellular resolution in cardiac muscles (Cheng and Lederer, 2008). However, it was studies of permeabilized cells ('skinned' fibres) that provided the first evidence for CICR in muscle (Endo et al., 1970; Fabiato and Fabiato, 1979). Analyses of RyRs that were reconstituted into planar lipid bilayers first showed that RyRs form large-conductance cation channels that are biphasically regulated by cytosolic Ca^{2+} (Lai et al., 1988; Meissner, 2017). Finally, analyses of RyR fragments by X-ray crystallography (Van Petegem, 2014) and of complete RyRs by cryo-electron microscopy (des Georges et al., 2016; Efremov et al., 2015; Peng et al., 2016; Yan et al., 2015; Zalk et al., 2015) are revealing the structural basis of RyR behaviour.

Progress towards understanding the second major family of intracellular Ca^{2+}-release channels, the IP_3Rs, began with an influential review in which a causal link between receptor-stimulated turnover of phosphatidylinositol and Ca^{2+} signalling was proposed (Michell, 1975). Subsequent work established that many receptors stimulate phospholipases C, which

cleave phosphatidylinositol 4,5-bisphosphate to produce IP_3 and diacylglycerol (Berridge, 1993) (**Fig. 1A**). IP_3 provides the link to Ca^{2+} signalling; not, as first envisaged by directly stimulating Ca^{2+} entry across the PM (Michell, 1975), but by stimulating Ca^{2+} release from the endoplasmic reticulum (ER) through IP_3Rs (Berridge and Irvine, 1984; Streb et al., 1983). Another influential review suggested the link between IP_3-evoked Ca^{2+} release and Ca^{2+} entry across the PM. This review proposed that loss of Ca^{2+} from the ER stimulated Ca^{2+} entry (Putney, 1986). The workings of this store-operated Ca^{2+} entry (SOCE) pathway are now clear: dissociation of Ca^{2+} from the luminal EF-hand motif of a protein embedded in the ER membrane, stromal interaction molecule 1 (STIM1), causes STIM1 to oligomerize and expose a cytosolic domain, through which it stimulates opening of a Ca^{2+}-selective channel in the PM (Feske et al., 2006; Prakriya and Lewis, 2015). The Ca^{2+} channel that mediates SOCE is a hexameric assembly of Orai subunits (Hou et al., 2012; Yen and Lewis, 2018), grandiloquently named from Greek mythology after the keepers of Heaven (Feske et al., 2006).

IP_3Rs and RyRs are biphasically regulated by cytosolic Ca^{2+} (Bezprozvanny et al., 1991). For IP_3Rs exposed to IP_3, a modest increase in $[Ca^{2+}]_c$ stimulates opening, whereas higher $[Ca^{2+}]_c$ are inhibitory (Foskett et al., 2007; Iino, 1990). Hence IP_3Rs, at least once they have bound IP_3 (Alzayady et al., 2016), can, like RyRs, mediate CICR (**Fig. 1B,C**). As with RyRs, IP_3Rs assemble into clusters, within which opening of one IP_3R ignites the activity of its neighbours to generate local 'Ca^{2+} puffs' (**Fig. 1C**) (Smith and Parker, 2009; Thillaiappan et al., 2017), analogous to Ca^{2+} sparks in muscle. These behaviours illustrate some of the many similarities between IP_3Rs and RyRs, which include their close structural relationship (Baker et al., 2017; Seo et al., 2012; Van Petegem, 2014). Although IP_3Rs and RyRs are the major intracellular Ca^{2+}-release channels, they are not the only intracellular Ca^{2+} channels (**Box 1**).

The productive interplay between studies of minimally perturbed tissue, facilitated by a plethora of Ca^{2+} indicators (Lock et al., 2015), fluorescent proteins (Rodriguez et al., 2017) and fluorescence microscopy techniques (Thorn, 2016), alongside analyses of cellular components has shaped our understanding of Ca^{2+} signalling. Here, we consider how analyses of IP_3Rs conducted outside their normal intracellular environment (*ex cellula*) have advanced our understanding of IP_3-evoked Ca^{2+} signals. We begin by considering how analyses of permeabilized cells established that the ER is the major intracellular Ca^{2+} store and that IP_3 releases Ca^{2+} from it. Radioligand binding analyses then both identified the sites to which IP_3 binds to activate IP_3Rs and paved the way to structural studies, which we show are now coming close to revealing how IP_3 binding causes the pore of the IP_3R to open. We

conclude by considering the contributions of electrophysiological recordings to our understanding of IP_3R gating.

Lessons from permeabilized cells

Permeabilized cells allow the Ca^{2+} content of intracellular organelles to be measured under conditions where the intracellular environment can be precisely controlled. To achieve this control, the PM must be disrupted without unduly perturbing organelles (Schulz, 1990). The permeabilized cells are then bathed in medium that mimics cytosol, notably in its low $[Ca^{2+}]_c$ (~100 nM). Electroporation (Knight, 1981; Xie et al., 2013) and a variety of chemical means have been used to selectively permeabilize the PM. The chemicals achieve their PM-selectivity by interacting with cholesterol (e.g. saponin, digitonin, β-escin), which is enriched in the PM (Wassler et al., 1987), or as pore-forming toxins (e.g. α-toxin, streptolysin-O) that are too large to pass through their own pores (Schulz, 1990).

After a protracted controversy (Babcock et al., 1979; Dehaye et al., 1980), analyses of permeabilized cells established that the ER, rather than mitochondria, is the major intracellular Ca^{2+} store in animal cells (Burgess et al., 1983). In an elegant study, saponin-permeabilized hepatocytes were bathed in cytosol-like medium with Ca^{2+} buffered to mimic the $[Ca^{2+}]_c$ of an unstimulated cell. Each permeabilized cell was then shown to have the same Ca^{2+} content as an intact cell, and critically all of that Ca^{2+} was in the ER (Burgess et al., 1983). Hence, it is the ER from which most extracellular stimuli evoke Ca^{2+} release.

Analyses of insect salivary glands demonstrated that phosphoinositide turnover was required for extracellular stimuli to evoke Ca^{2+} signals (Berridge and Fain, 1979), and showed that IP_3 was the first cytosolic product of receptor-stimulated phosphoinositide hydrolysis (Berridge, 1983). Hence, IP_3 emerged as the likely messenger that links receptors in the PM to Ca^{2+} release from the ER (**Fig. 1A**). Permeabilized cells again provided the decisive experiment: addition of IP_3 to permeabilized pancreatic acinar cells stimulated release of Ca^{2+} from a non-mitochondrial Ca^{2+} store (Streb et al., 1983). It is now universally accepted that most IP_3Rs reside in ER membranes, but IP_3Rs can also mediate Ca^{2+} release from the Golgi apparatus (Aulestia et al., 2015; Pinton et al., 1998), the nuclear envelope (Foskett et al., 2007; Rahman et al., 2009; Stehno-Bittel et al., 1995) and perhaps from a nucleoplasmic reticulum (Echevarria et al., 2003). In some cells, a few IP_3Rs (typically only 2-3 IP_3Rs per cell) are also expressed in the PM, where they mediate Ca^{2+} entry (Dellis et al., 2006; Dellis et al., 2008). In many studies, though not in all (Watras et al., 1991), the ER Ca^{2+} release evoked by IP_3 was shown to be positively cooperative (eg, Champeil et al., 1989; Marchant and Taylor,

1997; Meyer et al., 1988), suggesting a need for IP_3 to bind to several IP_3R subunits before the channel can open. A recent study using concatenated IP_3R subunits showed that a defective IP_3-binding site in only one of the four subunits prevents IP_3R activation (Alzayady et al., 2016), leading to the conclusion that all four subunits of an IP_3R must bind IP_3 before the channel can open.

But IP_3 binding is not alone sufficient to stimulate Ca^{2+} release through IP_3Rs. Instead, IP_3 binding primes IP_3Rs to bind Ca^{2+}, and Ca^{2+} binding then causes the channel to open (Adkins and Taylor, 1999; Marchant and Taylor, 1997) (**Fig. 1B**). Hence, IP_3Rs require binding of two ligands, IP_3 and Ca^{2+}, to open. This dual regulation endows IP_3Rs with their capacity to mediate regenerative Ca^{2+} signals through CICR. Again, it was analyses of permeabilized cells that provided the first evidence that Ca^{2+} release through IP_3Rs is regulated by $[Ca^{2+}]_c$ (Iino, 1987). High-resolution optical analyses of Ca^{2+} signals later revealed that within intact cells, IP_3-evoked Ca^{2+} signals originate from elementary units that comprise a small cluster of IP_3Rs (Smith and Parker, 2009; Thillaiappan et al., 2017). Opening of the first IP_3R within a cluster is proposed to rapidly ignite the activity of some of its neighbours by CICR to generate a Ca^{2+} puff (**Fig. 1C**). As the stimulus intensity increases, Ca^{2+} spreading from one Ca^{2+} puff to another IP_3R cluster can initiate further Ca^{2+} puffs, allowing the signal to spread across the cell as a regenerative Ca^{2+} wave (Marchant et al., 1999). The frequency of these global signals then increases with stimulus intensity (Thurley et al., 2014).

Structure-activity relationships (SAR), established by comparing the activities of a range of structurally-related chemical stimuli, are often used to probe the recognition properties of receptors. SAR analyses of the effects of IP_3 analogues on Ca^{2+} release from permeabilized cells provided the first evidence that dephosphorylation of IP_3 to (1,4)IP_2 terminates IP_3 activity (Burgess et al., 1984). The (1,3,4,5)IP_4 that is produced when IP_3 is phosphorylated by IP_3 3-kinase was proposed to regulate IP_3Rs (Loomis-Husselbee et al., 1996), but it is now clear that this phosphorylation also inactivates IP_3 signalling through IP_3Rs (Bird and Putney, 1996; Saleem et al., 2012). Hence, both endogenous pathways for IP_3 metabolism effectively inactivate IP_3 signalling to IP_3Rs (**Fig. 1A**). SAR analyses of many analogues of IP_3 and adenophostin A, a fungal metabolite that binds with high-affinity to IP_3Rs (Takahashi et al., 1994), established that a key feature of IP_3R agonists is the presence of a vicinal 4,5-bisphosphate moiety (**Fig. 1D**) (Rossi et al., 2010; Rossi et al., 2009; Saleem et al., 2012). All active inositol phosphate analogues have this 4,5-vicinal bisphosphate moiety (**Fig. 1D**).

There are no wholly selective antagonists of IP_3Rs. Some ligands (heparin, 2-aminoethoxydiphenylborane (2-APB), Xestospongin C and caffeine) have utility, but they all

lack selectivity. Furthermore, heparin is not membrane-permeant, and results with Xestospongin C are inconsistent (see Saleem et al., 2014). Addition of large substituents to the 2-*O*-position of IP_3 produces partial agonists. Partial agonists are ligands that, once they have bound to IP_3R, are less effective in causing the channel to open than full agonists like IP_3 (Rossi et al., 2009). These SAR analyses of 2-modified analogues of IP_3, again relying heavily on permeabilized cells, have both confirmed the importance of the extreme N-terminal region of the IP_3R (the suppressor domain, SD, **Fig. 1E**) in IP_3R activation and they suggest systematic strategies towards developing high-affinity antagonists of IP_3Rs.

There is, therefore, a long history of experiments using permeabilized cells illuminating our understanding of IP_3-evoked Ca^{2+} release. These studies first identified ER as the major intracellular Ca^{2+} store, they showed that IP_3 evokes Ca^{2+} release from the ER, and that IP_3Rs are regulated by Ca^{2+}. Furthermore, they defined the biochemical steps that inactivate IP_3 and, through SAR analyses, they have provided ligands that have contributed to understanding the mechanisms of IP_3R activation.

Analyses of IP_3 binding to IP_3Rs

Binding of IP_3 to the four binding sites of the IP_3R initiates the conformational changes that culminate in opening of the Ca^{2+}-permeable pore (Alzayady et al., 2016; Chandrasekhar et al., 2016). These IP_3 binding events are usually analysed by means of radioligand binding, which allows determination of binding affinities (as equilibrium dissociation constants, K_D) for ^3H-IP_3 or any competing ligand, but there are a variety of other methods (**Fig. 2, Box 2**). K_D values are important for comparison with functional analyses in revealing how ligands activate IP_3Rs. Such analyses were, for example, critical in showing that the vicinal 4,5-bisphosphate of IP_3 is essential for activity, whereas the 1-phosphate improves binding affinity (**Fig. 1D**) (Nahorski and Potter, 1989). Comparisons of SAR with binding analyses can also establish which bound ligands most effectively open the channel. Our comparisons of functional and ^3H-IP_3 equilibrium-competition binding analyses, for example, established that whereas IP_3 is a full agonist that effectively gates the IP_3R, other modified analogues of IP_3 bind with high-affinity to IP_3R, but they are much less effective in causing the channel to open (Rossi et al., 2009). These partial agonists provide insight into the mechanisms of IP_3R activation by demonstrating how large moieties at the 2-position of IP_3 attenuate IP_3R activation, and they suggest strategies for development of analogues that bind without activating IP_3Rs (i.e. antagonists).

Binding analyses also allow IP_3R properties to be addressed under conditions where IP_3-evoked Ca^{2+} release is not retained. This opportunity is particularly important during purification of IP_3Rs for structural studies using either IP_3R fragments for X-ray crystallography (Bosanac et al., 2002; Bosanac et al., 2005; Hamada et al., 2017; Lin et al., 2011; Seo et al., 2012) or, after detergent-solubilization of complete IP_3Rs, for single-particle analysis by cryo-EM (Fan et al., 2015; Paknejad and Hite, 2018). In subsequent sections, we review progress towards understanding how IP_3 binding leads to opening of the IP_3R pore.

IP_3 initiates IP_3R activation by binding to the IP_3-binding core

The route to IP_3R structures began with the identification of specific, high-affinity, intracellular ^{32}P-IP_3-binding sites with recognition properties that matched those expected of the receptor through which IP_3 evoked Ca^{2+} release (Baukal et al., 1985; Spät et al., 1986). Subsequent studies established that heparin competed with ^{3}H-IP_3 for these binding sites (heparin is a competitive antagonist of IP_3), and that the sites were abundant in Purkinje cells of cerebellum (Worley et al., 1987). Together, these observations allowed IP_3Rs to be purified from cerebellum using heparin-chromatography (Maeda et al., 1988; Supattapone et al., 1988). Functional reconstitution of the purified protein then established that it was alone sufficient to form an IP_3-gated Ca^{2+} channel (Ferris et al., 1989; Maeda et al., 1991). Many additional proteins were later shown to associate with IP_3Rs and modulate their responses to IP_3 (Prole and Taylor, 2016). Screening of cDNA libraries from cerebellum then provided the complete primary sequence of IP_3R1 (Furuichi et al., 1989; Mignery et al., 1989), and soon afterwards the other two IP_3R subtypes, IP_3R2 (Südhof et al., 1991) and IP_3R3 (Blondel et al., 1993) were identified. Subsequent studies established that the three IP_3R subunits (IP_3R1-3) assemble to form homo-tetrameric and hetero-tetrameric channels (Monkawa et al., 1995), and they confirmed that the core properties of all IP_3R subtypes are similar: each forms a large-conductance Ca^{2+}-permeable channel that is gated by binding of IP_3 and Ca^{2+} (Foskett, 2010), and each generates Ca^{2+} puffs (Mataragka and Taylor, 2018). The subtypes are, however, differentially expressed, and they differ in their affinities for IP_3 (Iwai et al., 2007), sensitivity to Ca^{2+} regulation (Foskett, 2010) and in whether they are modulated by additional regulators (Prole and Taylor, 2016). Furthermore, the functional consequences of mutant or defective IP_3Rs differ among subtypes (see Terry et al., 2018). IP_3R1 has so far been the major focus of the structural studies.

Deletion analyses (Mignery and Südhof, 1990) and expression of IP_3R fragments in bacteria (Yoshikawa et al., 1996) established that each IP_3R subunit has a single IP_3-binding site

237 formed by residues, the IBC (residues 224-604), towards the N-terminal of the primary
238 sequence (~2750 residues) (**Fig. 1E**). The identification of four IP_3-binding sites in each
239 IP_3R, and the demonstration that all four are required for IP_3 to evoke Ca^{2+} release (Alzayady
240 et al., 2016), provided an explanation for the widely observed cooperative responses to IP_3
241 (Champeil et al., 1989; Meyer et al., 1988; Parker and Miledi, 1989). Subsequent studies
242 identified residues within the IBC that are required for IP_3 binding, notably the residues that
243 bind to the critical 4- and 5-phosphate groups of IP_3 (Furutama et al., 1996). These residues
244 are conserved in IP_3Rs, but not in RyRs (Bosanac et al., 2002; Seo et al., 2012). It was also
245 shown that the SD inhibits IP_3 binding (Uchida et al., 2003), which aligns with the
246 importance of the SD in coupling IP_3 binding to channel gating (Rossi et al., 2009): IP_3Rs
247 without an SD bind IP_3 with high affinity, but they do not release Ca^{2+} (Uchida et al., 2003).
248 High-resolution crystal structures of N-terminal fragments of the IP_3R directly revealed both
249 the determinants of IP_3 binding and the initial steps in IP_3R activation. The two domains (α
250 and β) of the IBC form a clam-like structure, within which conserved residues bind to IP_3
251 (Bosanac et al., 2002). The 1- and 5-phosphates of IP_3 interact predominantly with residues in
252 IBC-α, whereas the 4-phosphate interacts with IBC-β (**Fig. 1D,E**). Interaction of the critical
253 4- and 5-phosphates with opposing sides of the clam allows IP_3 to partially close the clam and
254 initiate IP_3R activation (Hamada et al., 2017; Lin et al., 2011; Paknejad and Hite, 2018; Seo
255 et al., 2012). That interpretation, which elegantly reveals the structural basis of the SAR, is
256 supported by results with an adenophostin A analogue in which an alternative contact with
257 the α-domain substitutes for loss of the usual phosphate (Sureshan et al., 2012).
258 In the isolated N-terminal domain, the SD is firmly anchored to IBC-α by an extensive
259 interface and more loosely associated with IBC-β (**Fig. 1E**). Hence, when IP_3 causes the IBC
260 clam to close, the SD moves with IBC-α and that was predicted to disrupt interaction of an
261 exposed SD loop, the 'hot spot' loop (Yamazaki et al., 2010) with IBC-β of a neighbouring
262 subunit (Seo et al., 2012). In RyR too, these inter-subunit interactions between N-terminal
263 domains are weakened during receptor activation (des Georges et al., 2016). The resulting
264 weakening of interactions between subunits may contribute to channel gating. This is
265 supported by evidence that Ca^{2+}-binding protein 1 (CaBP1), which inhibits IP_3R gating,
266 rigidifies these interactions between IP_3R subunits (Li et al., 2013). However, within the
267 constraints of a full-length IP_3R, strong inter-subunit interactions between the SD and IBC-β
268 might constrain the SD, such that IBC-α moves when IP_3 closes the clam (Paknejad and Hite,
269 2018). Identification of the sites to which IP_3 binds, which relied heavily on radioligand

binding analyses, set the scene for the structural analyses that seek to understand how IP_3 binding opens the pore of the IP_3R. We consider recent progress with such structural analyses in the next section.

Structures of complete IP_3 and ryanodine receptors

Structures determined by single-particle analysis of cryo-EM images of the complete IP_3R1 in a closed state (Fan et al., 2015), of IP_3R3 with and without IP_3 and Ca^{2+} bound (Paknejad and Hite, 2018), and of RyRs in different states (des Georges et al., 2016; Efremov et al., 2015; Peng et al., 2016; Yan et al., 2015; Zalk et al., 2015) have begun to reveal the workings of the pore regions of these related channels. The results also tentatively suggest how IP_3 binding might lead to opening of the IP_3R pore.

The IP_3R has a structure reminiscent of a square mushroom. Much of the stalk is embedded in the ER membrane and the cap, with a diameter of ~25 nm, extends at least 13 nm into the cytosol (Fan et al., 2015). The large size is significant because it might exclude IP_3Rs from the narrow junctions between ER and the PM (Thillaiappan et al., 2017), whereas at other junctions, between ER and mitochondria for example (Csordas et al., 2018), it places the head of the IP_3R, from which Ca^{2+} exits, very close to the neighbouring organelle.

The cytosolic entrance to the central cavity of the IP_3R is surrounded by the N-terminal domains (SD and IBC-β, **Fig. 3**). IBC-α forms part of a larger domain (ARM1) that curves to the edge of the cap and interacts with two large curved domains (ARM2 and ARM3) that comprise most of the remaining cytosolic structure and form the underside of the mushroom (**Fig. 3**). Within the ER membrane, there are 24 trans-membrane domains (TMDs), six from each subunit (Fan et al., 2015). However, recent structural analyses of both IP_3R (Paknejad and Hite, 2018) and RyR1 (des Georges et al., 2016) identified a pair of additional helices (between TMD1 and 2 of IP_3R3) that challenge the accepted view that there are six TMDs per subunit. The TMD region, similar in structure to voltage-gated ion channels, is very similar (though not identical) (Baker et al., 2017) in RyRs and IP_3Rs. The ion-conducting path is lined by the four tilted TMD6 helices and a short (~1 nm) 'selectivity filter' at the luminal end through which hydrated cations must pass in single-file. The selectivity filter, its supporting pore-loop helix and a flexible luminal loop are all formed by residues linking TMD5 to TMD6. Near the cytosolic end of TMD6, a narrow hydrophobic constriction blocks the movement of ions in the closed channel (Fan et al., 2015) **(Fig. 3**). The hydrophobic side chains of these residues must move for the pore to open. Opening of the RyR is associated with splaying and bowing of TMD6, such that the hydrophobic side-chain of a residue that

occludes the cytosolic end of the closed pore is displaced, opening a hydrophilic path that allows passage of a hydrated Ca^{2+} ion. Similar mechanisms may be associated with opening of the IP_3R pore.

TMD6 is supported by TMD5, which is buttressed by the TMD1-4 bundle of the adjacent subunit. The short cytosolic TMD4-5 helical linker aligns along the ER membrane behind the TMD6 helices holding them in place. In the closed RyR1 channel, this linker tightly encircles the cytosolic end of the TMD6 bundle restricting its movement, but this grip is relaxed as the channel opens freeing TMD6 to move, and allowing the pore to dilate (des Georges et al., 2016). In both IP_3R and RyR, TMD6 extends well beyond the ER membrane (~1.5 nm in IP_3R) and then terminates in a pair of short α-helices (the linker domain, LNK, in IP_3R) that includes a Zn^{2+}-finger motif that aligns parallel with the ER membrane (des Georges et al., 2016; Fan et al., 2015; Paknejad and Hite, 2018). In IP_3R, but notably not in RyR, the entwined TMD6 helices then continue beyond the LNK domain to the cap of the mushroom, where each contacts the IBC-β domain of a neighbouring subunit (Fan et al., 2015). Hence, structures formed by the TMD5-6 loop guard the luminal entrance to the pore, whereas the cytosolic vestibule is formed by the extended TMD6. Each of these regions is enriched in acidic residues that probably contribute to the cation selectivity of IP_3R and RyR (des Georges et al., 2016; Fan et al., 2015; Paknejad and Hite, 2018).

A conserved Ca^{2+}-binding site is present in both RyR (des Georges et al., 2016) and IP_3R (Paknejad and Hite, 2018). The site is formed, in the case of IP_3R, by residues near the C-terminal end of ARM3 and by another residue contributed by the LNK domain (**Fig. 3**). In RyR, the equivalent residues are proposed to coordinate the Ca^{2+} required for stimulation (des Georges et al., 2016). The same may hold true for IP_3Rs, but this has yet to be tested. A conserved glutamate residue on the bottom surface of the ARM3 domain (Glu^{2101} in IP_3R1) previously suggested to mediate Ca^{2+} regulation of IP_3R (Miyakawa et al., 2001) and RyR (Fessenden et al., 2001), does not contribute to Ca^{2+} binding to this site, but it does stabilize the interaction between the cooperating domains in RyR1 (des Georges et al., 2016). A second Ca^{2+}-binding site was identified in the structure of IP_3R3, and again it is formed by residues that are contributed by different domains (ARM3 and the α-helical domain linking ARM1 to ARM2) (Paknejad and Hite, 2018) (**Fig. 3**). Formation of both Ca^{2+}-binding sites requires movement of the contributing domains from their positions in the apo-state, so as to bring the Ca^{2+}-coordinating residues into register (Paknejad and Hite, 2018). This important observation is consistent with evidence that IP_3 controls IP_3R gating by regulating Ca^{2+} binding (**Fig. 1B**).

Taken together, structures of full-length IP_3Rs have defined where IP_3 binds, identified Ca^{2+}-binding sites that may mediate Ca^{2+} regulation, and established that hydrophobic residues projecting into the pore must move to allow Ca^{2+} to pass.

Towards understanding how IP_3 and Ca^{2+} binding open the IP_3R pore

The only contacts between the large cytosolic structures of the IP_3R and its channel region are the C-terminal end of ARM3 and the LNK domain (**Fig. 3**) (Fan et al., 2015). There are similar contacts in RyR (des Georges et al., 2016). In both IP_3R and RyR, this critical nexus comprises a platform of interleaved structures: the C-terminus of the ARM3 domain (the intervening lateral domain, ILD) forms a 'thumb-and-fingers' arrangement of an upper thumb abutting the bulk of ARM3, and an α-helical pair of fingers lying below and forming a cavity into which the LNK domain inserts (**Fig. 3**) (Fan et al., 2015). Mutations within the thumb disrupt IP_3R function (Hamada et al., 2017). The LNK domain also wraps around the thumb and contributes a residue to the Ca^{2+}-binding site at the base of the ARM3 domain.

How, then, does IP_3 binding to the IBC cause hydrophobic pore residues some 7 nm distant to move and allow Ca^{2+} to pass from the ER lumen to the cytosol (Fan et al., 2015)? Recalling that IP_3 primes IP_3Rs to bind Ca^{2+}, which then triggers channel opening (Adkins and Taylor, 1999) (**Fig. 1B**), it seems reasonable to speculate that IP_3 binding to the IBC is communicated to the Ca^{2+}-binding site at the ILD-LNK nexus and thence to the pore (Paknejad and Hite, 2018). IP_3 binding closes the clam-like IBC, and, with IBC-β held firmly in place by inter-subunit interactions at the top of the mushroom, IBC-α moves and initiates conformational changes throughout the associated ARM domains. These changes include disruption of inter-subunit interaction between ARM1 and ARM2 domains, and rotation of the LNK domains (Paknejad and Hite, 2018). Here, the need for the SD is attributed to its role in stabilizing inter-subunit interactions to provide a fixed structure against which movement of IBC-α can leverage conformational changes through the ARM domains (Paknejad and Hite, 2018).

Given the essential role of the SD in IP_3R activation, an alternative possibility was that the direct contact between the SD and ARM3 might mediate communication between N-terminal regions and the ILD. However, the SD-ARM3 interaction occurs through the handle of the hammer-like SD, which can be deleted without impairing IP_3R function (Yamazaki et al., 2010). Another possibility was that interaction between IBC-β and the CTD (which is unique to IP_3R) might communicate IP_3 binding to the LNK domain. However, this scheme is difficult to reconcile with functional IP_3R/RyR chimeras (Seo et al., 2012) since the RyR structure does not have an extended CTD, and with evidence that deletion of residues within

the CTD that interact with IBC-β do not prevent IP_3-evoked Ca^{2+} release (Hamada et al., 2017; Schug and Joseph, 2006). Whatever the exact path from IBC to the ILD-LNK nexus is, IP_3-evoked conformational changes appear to reconfigure the Ca^{2+}-binding site formed at the LNK-ARM3 interface to allow Ca^{2+} binding (Paknejad and Hite, 2018), thereby providing a plausible mechanism for IP_3 priming IP_3Rs to respond to Ca^{2+} (**Fig. 1B**).

We conclude that analyses of IP_3 binding contributed to defining the SAR for IP_3Rs and to quantitative comparisons of the relationship between binding and channel activation, but most significantly they allowed IP_3Rs to be identified during their purification, which paved the way to cloning and molecular manipulation of IP_3Rs, and to structural studies. The latter have established that IP_3Rs are huge tetrameric structures, wherein IP_3 binding closes a clam-like IBC. That conformational change is communicated to a critical nexus between interleaved structures from the cytosolic and channel domains. IP_3 binding probably stabilizes Ca^{2+} binding to this nexus, leading to re-arrangement of the pore, such that occluding hydrophobic residues are displaced to allow the passage of Ca^{2+} from the ER lumen to the cytosol.

Lessons from planar lipid bilayers and patch-clamp recording

Electrical recordings from ion channels, most often by means of patch-clamp recording (**Box 3**) (Lape et al., 2008; Neher, 1992), allow the openings and closing of single channels to be recorded with sub-millisecond resolution, and they allow their ion permeation properties to be defined. Since the intracellular location of RyR and IP_3R in the ER presents a formidable barrier to such recordings (Jonas et al., 1997), two alternative approaches have been used.

Planar lipid bilayers

The first approach, which involves reconstitution of ER vesicles or solubilized IP_3Rs into planar lipid bilayers, provided the first measurements of currents through IP_3R (Bezprozvanny et al., 1994; Bezprozvanny and Ehrlich, 1994; Bezprozvanny et al., 1991; Ehrlich and Watras, 1988; Maeda et al., 1991). These analyses established that IP_3R, like RyR, are large-conductance cation channels with relatively low-selectivity for Ca^{2+}. Both features are important in allowing IP_3R to generate large local cytosolic Ca^{2+} signals: the large conductance allows an open IP_3R to pass ~500,00 Ca^{2+} per second (Foskett et al., 2007), whereas the weak selectivity might allow a counter-flux of K^+ to dissipate the electrical gradient that is formed as Ca^{2+} leaves the ER and which would otherwise rapidly terminate Ca^{2+} release (Zsolnay et al., 2018). The short, wide selectivity filter and large vestibules with

abundant acidic residues probably provide the structural basis of these ion permeation properties (Fan et al., 2015). Bilayer analyses also confirmed the biphasic regulation of IP_3R1 by cytosolic Ca^{2+} (Bezprozvanny et al., 1991). A potential problem with recordings from planar lipid bilayers is that solubilization and/or reconstitution could lead to loss of accessory proteins or perturbation of structure. Maximal open probabilities recorded from IP_3Rs in bilayers, for example, are much lower than in patch-clamp recordings, and bilayer recordings of IP_3R2 and IP_3R3 failed to capture the inhibitory effect of cytosolic Ca^{2+} (Hagar et al., 1998; Ramos-Franco et al., 2000).

Patch-clamp recording

The second approach to obtaining electrical recordings from IP_3R exploits the fact that the ER is continuous with the outer nuclear membrane (ONM) (**Box 3**) (Dingwall and Laskey, 1992). Hence, patch-clamp recording from the ONM allows analysis of IP_3R in a native membrane, albeit not the ER (Mak et al., 2013; Rahman and Taylor, 2010) (**Box 3**). These recordings, which have been applied to both native and heterologously expressed IP_3Rs (Betzenhauser et al., 2008; Cheung et al., 2010; Foskett et al., 2007; Marchenko et al., 2005; Rahman et al., 2009), confirmed their ion permeation properties and the biphasic regulation of all IP_3R subtypes by Ca^{2+}. They have also suggested complex gating schemes wherein IP_3 drives bursts of IP_3R activity by extending the duration of sequences of openings and shortening the gaps between the bursts (Gin et al., 2009; Ionescu et al., 2007).

Another application of nuclear patch-clamp recording is provided by our work, where we showed that IP_3Rs within patches that fortuitously contained several IP_3Rs behave differently to patches with only a single IP_3R (Rahman et al., 2009). This led to our proposal that low concentrations of IP_3, perhaps arising from occupancy of only some of the four IP_3-binding sites, trigger IP_3R clustering (Rahman et al., 2009). The clustered IP_3Rs, we suggest, are better placed than lone IP_3Rs to benefit from CICR when a near neighbour opens to release Ca^{2+} and so provide the second stimulus that is needed for IP_3R opening (**Fig. 1B**). Effects of clustering on the IP_3 and Ca^{2+} sensitivity of IP_3Rs reinforce the propensity of clustered IP_3Rs to amplify Ca^{2+} signals by CICR. These proposals have been challenged (Rahman et al., 2011; Smith et al., 2009; Vais et al., 2011) and our own recent work suggests that even in unstimulated cells there are pre-existing clusters of IP_3Rs, each typically comprising about eight IP_3Rs (Thillaiappan et al., 2017). Our revised proposal therefore envisages that IP_3Rs are, as we have shown, loosely clustered in unstimulated cells (Thillaiappan et al., 2017) and

that IP_3 might then cause IP_3Rs within the cluster to huddle more closely and so be more likely to respond to Ca^{2+} released by a neighbour.

Concluding remarks

Throughout the long history of analyses of intracellular Ca^{2+} signalling, there has been a productive interplay between studies of intact tissues and of biological systems extracted from intact cells (*ex cellula*). These approaches succeeded in showing that the ER is the major intracellular Ca^{2+} store and they identified the enormous channels (RyR and IP_3R) that mediate Ca^{2+} release from the ER. We are now fast approaching an understanding of how IP_3 binding leads, through its interactions with Ca^{2+} binding, to opening of the IP_3R. In parallel with these approaches, developments in optical microscopy have provided opportunities to examine IP_3-evoked Ca^{2+} release with exquisite temporal and spatial resolution in intact cells. We can surely look forward to these analyses converging with structural analyses *in situ* to provide a comprehensive understanding of IP_3Rs in living cells.

Funding

This work was supported by the Wellcome Trust (grant number 101844) and the Biotechnology and Biological Sciences Research Council (grant number BB/P005330/1).

References

Adkins, C. E. and Taylor, C. W. (1999). Lateral inhibition of inositol 1,4,5-trisphosphate receptors by cytosolic Ca^{2+}. *Curr. Biol.* **9**, 1115-1118.

Alzayady, K. J., Wang, L., Chandrasekhar, R., Wagner, L. E., 2nd, Van Petegem, F. and Yule, D. I. (2016). Defining the stoichiometry of inositol 1,4,5-trisphosphate binding required to initiate Ca^{2+} release. *Sci. Signal.* **9**, ra35.

Aulestia, F. J., Alonso, M. T. and Garcia-Sancho, J. (2015). Differential calcium handling by the cis and trans regions of the Golgi apparatus. *Biochem. J.* **466**, 455-465.

Babcock, D. F., Chen, J. L., Yip, B. P. and Lardy, H. A. (1979). Evidence for mitochondrial localization of the hormone-responsive pool of Ca^{2+} in isolated hepatocytes. *J. Biol. Chem.* **254**, 8117-8120.

Baker, M. R., Fan, G. and Serysheva, II. (2017). Structure of IP_3R channel: high-resolution insights from cryo-EM. *Curr. Opin. Struct. Biol.* **46**, 38-47.

Baukal, A. J., Guillemette, G., Rubin, R., Spat, A. and Catt, K. J. (1985). Binding sites for inositol trisphosphate in the bovine adrenal cortex. *Biochem. Biophys. Res. Commun.* **133**, 532-538.

Berridge, M. J. (1983). Rapid accumulation of inositol trisphosphate reveals that agonists hydrolyse polyphosphoinositides instead of phosphatidylinositol. *Biochem. J.* **212**, 849-858.

Berridge, M. J. (1993). Inositol trisphosphate and calcium signalling. *Nature* **361**, 315-325.

Berridge, M. J. and Fain, J. N. (1979). Inhibition of phosphatidylinositol synthesis and the inactivation of calcium entry after prolonged exposure of the blowfly salivary gland to 5-hydroxytryptamine. *Biochem. J.* **178**, 59-69.

Berridge, M. J. and Irvine, R. F. (1984). Inositol trisphosphate, a novel second messenger in cellular signal transduction. *Nature* **312**, 315-321.

Bers, D. M. (2002). Cardiac excitation-contraction coupling. *Nature* **415**, 198-205.

Betzenhauser, M. J., Wagner, L. E., 2nd, Won, J. H. and Yule, D. I. (2008). Studying isoform-specific inositol 1,4,5-trisphosphate receptor function and regulation. *Methods* **46**, 177-82.

Bezprozvanny, I., Bezprozvannaya, S. and Ehrlich, B. E. (1994). Caffeine-induced inhibition of inositol(1,4,5)-trisphosphate-gated calcium channels from cerebellum. *Mol. Biol. Cell* **5**, 97-103.

Bezprozvanny, I. and Ehrlich, B. E. (1994). Inositol (1,4,5)-trisphosphate ($InsP_3$)-gated Ca channels from cerebellum: conduction properties for divalent cations and regulation by intraluminal calcium. *J. Gen. Physiol.* **104**, 821-856.

Bezprozvanny, I., Watras, J. and Ehrlich, B. E. (1991). Bell-shaped calcium-response curves for $Ins(1,4,5)P_3$- and calcium-gated channels from endoplasmic reticulum of cerebellum. *Nature* **351**, 751-754.

Bird, G. S. J. and Putney, J. W., Jr. (1996). Effect of inositol 1,3,4,5-trisphosphate on inositol trisphosphate-activated Ca^{2+} signaling in mouse lacrimal cells. *J. Biol. Chem.* **271**, 6766-6770.

Blondel, O., Takeda, J., Janssen, H., Seino, S. and Bell, G. I. (1993). Sequence and functional characterization of a third inositol trisphosphate receptor subtype, IP_3R-3, expressed in pancreatic islets, kidney, gastrointestinal tract, and other tissues. *J. Biol. Chem.* **268**, 11356-11363.

Bosanac, I., Alattia, J.-R., Mal, T. K., Chan, J., Talarico, S., Tong, F. K., Tong, K. I., Yoshikawa, F., Furuichi, T., Iwai, M. et al. (2002). Structure of the inositol 1,4,5-trisphosphate receptor binding core in complex with its ligand. *Nature* **420**, 696-700.

Bosanac, I., Yamazaki, H., Matsu-ura, T., Michikawa, T., Mikoshiba, K. and Ikura, M. (2005). Crystal structure of the ligand binding suppressor domain of type 1 inositol 1,4,5-trisphosphate receptor. *Mol. Cell* **17**, 193-203.

Burgess, G. M., Irvine, R. F., Berridge, M. J., McKinney, J. S. and Putney, J. W., Jr. (1984). Actions of inositol phosphates on calcium pools in guinea pig hepatocytes. *Biochem. J.* **224**, 741-746.

Burgess, G. M., McKinney, J. S., Fabiato, A., Leslie, B. A. and Putney, J. W., Jr. (1983). Calcium pools in saponin-permeabilized guinea pig hepatocytes. *J. Biol. Chem.* **258**, 15336-15345.

Cao, Q., Yang, Y., Zhong, X. Z. and Dong, X. P. (2017). The lysosomal Ca^{2+} release channel TRPML1 regulates lysosome size by activating calmodulin. *J. Biol. Chem.* **292**, 8424-8435.

Champeil, P., Combettes, L., Berthon, B., Doucet, E., Orlowski, S. and Claret, M. (1989). Fast kinetics of calcium release induced by myo-inositol trisphosphate in permeabilized rat hepatocytes. *J. Biol. Chem.* **264**, 17665-17673.

Chandrasekhar, R., Alzayady, K. J., Wagner, L. E., 2nd and Yule, D. I. (2016). Unique regulatory properties of heterotetrameric inositol 1,4,5-trisphosphate receptors revealed by studying concatenated receptor constructs. *J. Biol. Chem.* **291**, 4846-4860.

Cheng, H. and Lederer, W. J. (2008). Calcium sparks. *Physiol. Rev.* **88**, 1491-1545.

Cheng, Y.-C. and Prusoff, W. H. (1973). Relationship between the inhibition constant (K_I) and the concentration of inhibitor causing 50 per cent inhibition (IC_{50}) of an enzymatic reaction. *Biochem. Pharmacol.* **22**, 3099-3108.

Cheung, K. H., Mei, L., Mak, D. O., Hayashi, I., Iwatsubo, T., Kang, D. E. and Foskett, J. K. (2010). Gain-of-function enhancement of IP_3 receptor modal gating by familial Alzheimer's disease-linked presenilin mutants in human cells and mouse neurons. *Sci. Signal.* **3**, ra22.

Csordas, G., Weaver, D. and Hajnoczky, G. (2018). Endoplasmic reticular-mitochondrial contactology: structure and signaling functions. *Trends Cell Biol.* **28**, 523-540.

de Azevedo, W. F., Jr. and Dias, R. (2008). Experimental approaches to evaluate the thermodynamics of protein-drug interactions. *Curr. Drug Targets* **9**, 1071-1076.

Dehaye, J. P., Blackmore, P. F., Venter, J. C. and Exton, J. H. (1980). Studies on the alpha-adrenergic activation of hepatic glucose output. alpha-adrenergic activation of phosphorylase by immobilized epinephrine. *J. Biol. Chem.* **255**, 3905-3910.

Dellis, O., Dedos, S., Tovey, S. C., Rahman, T.-U.-., Dubel, S. J. and Taylor, C. W. (2006). Ca^{2+} entry through plasma membrane IP_3 receptors. *Science* **313**, 229-233.

Dellis, O., Rossi, A. M., Dedos, S. G. and Taylor, C. W. (2008). Counting functional IP_3 receptors into the plasma membrane. *J. Biol. Chem.* **283**, 751-755.

des Georges, A., Clarke, O. B., Zalk, R., Yuan, Q., Condon, K. J., Grassucci, R. A., Hendrickson, W. A., Marks, A. R. and Frank, J. (2016). Structural basis for gating and activation of RyR1. *Cell* **167**, 145-157.

Ding, Z., Rossi, A. M., Riley, A. M., Rahman, T., Potter, B. V. L. and Taylor, C. W. (2010). Binding of inositol 1,4,5-trisphosphate (IP_3) and adenophostin A to the N-terminal region of the IP_3 receptor: thermodynamic analysis using fluorescence polarization with a novel IP_3 receptor ligand. *Mol. Pharmacol.* **77**, 995-1004.

Dingwall, C. and Laskey, R. (1992). The nuclear membrane. *Science* **258**, 942-947.

Echevarria, W., Leite, M. F., Guerra, M. T., Zipfel, W. R. and Nathanson, M. H. (2003). Regulation of calcium signals in the nucleus by a nucleoplasmic reticulum. *Nat. Cell Biol.* **5**, 440-446.

Efremov, R. G., Leitner, A., Aebersold, R. and Raunser, S. (2015). Architecture and conformational switch mechanism of the ryanodine receptor. *Nature* **517**, 39-43.

Ehrlich, B. E. and Watras, J. (1988). Inositol 1,4,5-trisphosphate activates a channel from smooth muscle sarcoplasmic reticulum. *Nature* **336**, 583-586.

Endo, M., Tanaka, M. and Ogawa, Y. (1970). Calcium induced release of calcium from the sarcoplasmic reticulum of skinned skeletal muscle fibres. *Nature* **228**, 34-36.

Fabiato, A. and Fabiato, F. (1979). Use of chlorotetracycline fluorescence to demonstrate Ca^{2+}-induced release of Ca^{2+} from sarcoplasmic reticulum of skinned cardiac cells. *Nature* **281**, 146-148.

Fan, G., Baker, M. L., Wang, Z., Baker, M. R., Sinyagovskiy, P. A., Chiu, W., Ludtke, S. J. and Serysheva, I. I. (2015). Gating machinery of $InsP_3R$ channels revealed by electron cryomicroscopy. *Nature* **527**, 336-341.

Ferris, C. D., Huganir, R. L., Supattapone, S. and Snyder, S. H. (1989). Purified inositol 1,4,5-trisphosphate receptor mediates calcium flux in reconstituted lipid vesicles. *Nature* **342**, 87-89.

Feske, S., Gwack, Y., Prakriya, M., Srikanth, S., Puppel, S. H., Tanasa, B., Hogan, P. G., Lewis, R. S., Daly, M. and Rao, A. (2006). A mutation in Orai1 causes immune deficiency by abrogating CRAC channel function. *Nature* **441**, 179-185.

Fessenden, J. D., Chen, L., Wang, Y., Paolini, C., Franzini-Armstrong, C., Allen, P. D. and Pessah, I. N. (2001). Ryanodine receptor point mutant E4032A reveals an allosteric interaction with ryanodine. *Proc. Natl. Acad. Sci. USA* **98**, 2865-2870.

Foskett, J. K. (2010). Inositol trisphosphate receptor Ca^{2+} release channels in neurological diseases. *Pfluegers Arch./Eur. J. Physiol.* **460**, 481-494.

Foskett, J. K., White, C., Cheung, K. H. and Mak, D. O. (2007). Inositol trisphosphate receptor Ca^{2+} release channels. *Physiol. Rev.* **87**, 593-658.

Furuichi, T., Yoshikawa, S., Miyawaki, A., Wada, K., Maeda, M. and Mikoshiba, K. (1989). Primary structure and functional expression of the inositol 1,4,5-trisphosphate-binding protein P_{400}. *Nature* **342**, 32-38.

Furutama, D., Shimoda, K., Yoshikawa, S., Miyawaki, A., Furuichi, T. and Mikoshiba, K. (1996). Functional expression of the type 1 inositol 1,4,5-trisphosphate receptor promoter-*lacz* fusion genes in transgenic mice *J. Neurochem.* **66**, 1793-1801.

Gin, E., Falcke, M., Wagner, L. E., 2nd, Yule, D. I. and Sneyd, J. (2009). A kinetic model of the inositol trisphosphate receptor based on single-channel data. *Biophys. J.* **96**, 4053-4062.

Hagar, R. E., Burgstahler, A. D., Nathanson, M. H. and Ehrlich, B. E. (1998). Type III $InsP_3$ receptor channel stays open in the presence of increased calcium. *Nature* **296**, 81-84.

Hamada, K., Miyatake, H., Terauchi, A. and Mikoshiba, K. (2017). IP_3-mediated gating mechanism of the IP_3 receptor revealed by mutagenesis and X-ray crystallography. *Proc. Natl. Acad. Sci. USA* **114**, 4661-4666.

Hou, X., Pedi, L., Diver, M. M. and Long, S. B. (2012). Crystal structure of the calcium release-activated calcium channel Orai. *Science* **338**, 1308-1313.

Huang, P., Zou, Y., Zhong, X. Z., Cao, Q., Zhao, K., Zhu, M. X., Murell-Lagnado, R. and Dong, X. P. (2014). P2X4 forms functional ATP-activated cation channels on lysosomal membranes regulated by luminal pH. *J. Biol. Chem.* **289**, 17658-17667.

Iino, M. (1987). Calcium dependent inositol trisphosphate-induced calcium release in the guinea-pig taenia caeci. *Biochem. Biophys. Res. Commun.* **142**, 47-52.

Iino, M. (1990). Biphasic Ca^{2+} dependence of inositol 1,4,5-trisphosphate-induced Ca^{2+} release in smooth muscle cells of the guinea pig taenia caeci. *J. Gen. Physiol.* **95**, 1103-1122.

Ionescu, L., White, C., Cheung, K. H., Shuai, J., Parker, I., Pearson, J. E., Foskett, J. K. and Mak, D. O. (2007). Mode switching is the major mechanism of ligand regulation of $InsP_3$ receptor calcium release channels. *J. Gen. Physiol.* **130**, 631-635.

Iwai, M., Michikawa, T., Bosanac, I., Ikura, M. and Mikoshiba, K. (2007). Molecular basis of the isoform-specific ligand-binding affinity of inositol 1,4,5-trisphosphate receptors. *J. Biol. Chem.* **282**, 12755-12764.

Jonas, E. A., Knox, R. J. and Kaczmarek, L. (1997). Giga-ohm seals on intracellular membranes: a technique for studying intracellular ion channels in intact cells. *Neuron* **19**, 7-13.

Knight, D. E. (1981). Rendering cells permeable by exposure to electric fields. In *Techniques in Cellular Physiology*, pp. 1-20. Amsterdam: Elsevier/North Holland Scientific Publishers Ltd.

Koulen, P., Cai, Y., Geng, L., Maeda, Y., Nishimura, S., Witzgall, R., Ehrlich, B.E. and Somlo, S. (2002). Polycystin-2 is an intracellular calcium release channel. *Nat Cell Biol.* **4,**191-197.

Lai, F. A., Erickson, H. P., Rousseau, E., Liu, Q.-Y. and Meissner, G. (1988). Purification and reconsitution of the calcium release channel from skeletal muscle. *Nature* **331**, 315-319.

Lape, R., Colquhoun, D. and Sivilotti, L. G. (2008). On the nature of partial agonism in the nicotinic receptor superfamily. *Nature* **454**, 722-727.

Li, C., Enomoto, M., Rossi, A. M., Seo, M.-D., Rahman, T., Stathopulos, P. B., Taylor, C. W., Ikura, M. and Ames, J. B. (2013). CaBP1, a neuronal Ca^{2+} sensor protein, inhibits inositol trisphosphate receptors by clamping inter-subunit interactions. *Proc. Natl. Acad. Sci. USA* **110**, 8507-8512.

Lin, C. C., Baek, K. and Lu, Z. (2011). Apo and $InsP_3$-bound crystal structures of the ligand-binding domain of an $InsP_3$ receptor. *Nat. Struct. Mol. Biol.* **18**, 1172-1174.

Lock, J. T., Parker, I. and Smith, I. F. (2015). A comparison of fluorescent Ca^{2+} indicators for imaging local Ca^{2+} signals in cultured cells. *Cell Calcium* **58**, 638-648.

Loomis-Husselbee, J. W., Cullen, P. J., Dreikhausen, U. E., Irvine, R. F. and Dawson, A. P. (1996). Synergistic effects of inositol 1,3,4,5-tetrakisphosphate on inositol 2,4,5-trisphosphate-stimulated Ca^{2+} release do not involve direct interaction of inositol

1,3,4,5-tetrakisphosphate with inositol trisphosphate-binding sites. *Biochem. J.* **314**, 811-816.

Ludtke, S. J., Serysheva, I. I., Hamilton, S. L. and Chiu, W. (2005). The pore structure of the closed RYR1 channel. *Structure* **13**, 1203-1211.

Ludtke, S. J., Tran, T. P., Ngo, Q. T., Moiseenkova-Bell, V. Y., Chiu, W. and Serysheva, I. I. (2011). Flexible architecture of IP_3R1 by cryo-EM. *Structure* **19**, 1192-1199.

Maeda, N., Kawasaki, T., Nakade, S., Yokota, N., Taguchi, T., Kasai, M. and Mikoshiba, K. (1991). Structural and functional characterization of inositol 1,4,5-trisphosphate receptor channel from mouse cerebellum. *J. Biol. Chem.* **266**, 1109-1116.

Maeda, N., Niinobe, M., Nakahira, K. and Mikoshiba, K. (1988). Purification and characterization of P_{400} protein, a glycoprotein characteristic of purkinje cell from mouse cerebellum. *J. Neurochem.* **51**, 1724-1730.

Mak, D. O. and Foskett, J. K. (2014). Inositol 1,4,5-trisphosphate receptors in the endoplasmic reticulum: A single-channel point of view. *Cell Calcium* **58**, 67-78.

Mak, D. O., Pearson, J. E., Loong, K. P., Datta, S., Fernandez-Mongil, M. and Foskett, J. K. (2007). Rapid ligand-regulated gating kinetics of single inositol 1,4,5-trisphosphate receptor Ca^{2+} release channels. *EMBO Rep.* **8**, 1044-1051.

Mak, D. O., Vais, H., Cheung, K. H. and Foskett, J. K. (2013). Patch-clamp electrophysiology of intracellular Ca^{2+} channels. *Cold Spring Harbor Protocols* **2013**, 787-97.

Marchant, J., Callamaras, N. and Parker, I. (1999). Initiation of IP_3-mediated Ca^{2+} waves in *Xenopus* oocytes. *EMBO J.* **18**, 5285-5299.

Marchant, J. S. and Taylor, C. W. (1997). Cooperative activation of IP_3 receptors by sequential binding of IP_3 and Ca^{2+} safeguards against spontaneous activity. *Curr. Biol.* **7**, 510-518.

Marchenko, S. M., Yarotskyy, V. V., Kovalenko, T. N., Kostyuk, P. G. and Thomas, R. C. (2005). Spontaneously active and $InsP_3$-activated ion channels in cell nuclei from rat cerebellar Purkinje and granule neurones. *J. Physiol.* **565**, 897-910.

Mataragka, S. and Taylor, C. W. (2018). All three IP_3 receptor subtypes generate Ca^{2+} puffs, the universal building blocks of IP_3-evoked Ca^{2+} signals. *J. Cell Sci.* **In press**.

Meissner, G. (2017). The structural basis of ryanodine receptor ion channel function. *J. Gen. Physiol.* **149**, 1065-1089.

Meyer, T., Holowka, D. and Stryer, L. (1988). Highly cooperative opening of calcium channels by inositol 1,4,5-trisphosphate. *Science* **240**, 653-656.

Michell, R. H. (1975). Inositol phospholipids and cell surface receptor function. *Biochim. Biophys. Acta* **415**, 81-147.

Mignery, G. A. and Südhof, T. C. (1990). The ligand binding site and transduction mechanism in the inositol-1,4,5-trisphosphate receptor. *EMBO J.* **9**, 3893-3898.

Mignery, G. A., Südhof, T. C., Takei, K. and De Camilli, P. (1989). Putative receptor for inositol 1,4,5-trisphosphate similar to ryanodine receptor. *Nature* **342**, 192-195.

Miyakawa, T., Mizushima, A., Hirose, K., Yamazawa, T., Bezprozvanny, I., Kurosaki, T. and Iino, M. (2001). Ca^{2+}-sensor region of IP_3 receptor controls intracellular Ca^{2+} signaling. *EMBO J.* **20**, 1674-1680.

Monkawa, T., Miyawaki, A., Sugiyama, T., Yoneshima, H., Yamamoto-Hino, M., Furuichi, T., Saruta, T., Hasagawa, M. and Mikoshiba, K. (1995). Heterotetrameric complex formation of inositol 1,4,5-trisphosphate receptor subunits. *J. Biol. Chem.* **270**, 14700-14704.

Morgan, A. J. and Galione, A. (2013). Two-pore channels (TPCs): current controversies. *Bioessays* **36**, 173-183.

Nahorski, S. R. and Potter, B. V. L. (1989). Molecular recognition of inositol polyphosphates by intracellular receptors and metabolic enzymes. *Trends Pharmacol. Sci.* **10**, 139-144.

Neher, E. (1992). Nobel lecture. Ion channels for communication between and within cells. *EMBO J.* **11**, 1672-1679.

Oxenoid, K., Dong, Y., Cao, C., Cui, T., Sancak, Y., Markhard, A. L., Grabarek, Z., Kong, L., Liu, Z., Ouyang, B. et al. (2016). Architecture of the mitochondrial calcium uniporter. *Nature* **533**, 269-273.

Paknejad, N. and Hite, R. K. (2018). Structural basis for the regulation of inositol trisphosphate receptors by Ca^{2+} and IP_3. *Nat. Struct. Mol. Biol.* **25**, 660-668.

Parker, I. and Miledi, R. (1989). Nonlinearity and facilitation in phosphoinositide signaling studied by the use of caged inositol trisphosphate in *Xenopus* oocytes. *J. Neurosci.* **9**, 4068-4077.

Patel, S., Harris, A., O'Beirne, G., Cook, N. D. and Taylor, C. W. (1996). Kinetic analysis of inositol trisphosphate binding to pure inositol trisphosphate receptors using scintillation proximity assay. *Biochem. Biophys. Res. Commun.* **221**, 821-825.

Patron, M., Raffaello, A., Granatiero, V., Tosatto, A., Merli, G., De Stefani, D., Wright, L., Pallafacchina, G., Terrin, A., Mammucari, C. et al. (2013). The mitochondrial

calcium uniporter (MCU): molecular identity and physiological roles. *J. Biol. Chem.* **288**, 10750-10758.

Peng, W., Shen, H., Wu, J., Guo, W., Pan, X., Wang, R., Chen, S. R. and Yan, N. (2016). Structural basis for the gating mechanism of the type 2 ryanodine receptor RyR2. *Science* **354**, aah5324.

Pinton, P., Pozzan, T. and Rizzuto, R. (1998). The Golgi apparatus is an inositol 1,4,5-trisphosphate-sensitive Ca^{2+} store, with functional properties distinct from those of the endoplasmic reticulum. *EMBO J.* **17**, 5298-5308.

Prakriya, M. and Lewis, R. S. (2015). Store-operated calcium channels. *Physiol. Rev.* **95**, 1383-1436.

Prole, D. L. and Taylor, C. W. (2016). Inositol 1,4,5-trisphosphate receptors and their protein partners as signalling hubs. *J. Physiol.* **594**, 2849-2866.

Putney, J. W., Jr. (1986). A model for receptor-regulated calcium entry. *Cell Calcium* **7**, 1-12.

Rahman, T., Skupin, A., Falcke, M. and Taylor, C. W. (2011). $InsP_3R$ channel gating altered by clustering? Rahman *et al.* reply. *Nature* **478**, E2-E3.

Rahman, T. and Taylor, C. W. (2010). Nuclear patch-clamp recording from inositol 1,4,5-trisphosphate receptors. In *Calcium in Living Cells*, (ed. M. Whittaker), pp. 199-224. Amsterdam: Elsevier.

Rahman, T. U., Skupin, A., Falcke, M. and Taylor, C. W. (2009). Clustering of IP_3 receptors by IP_3 retunes their regulation by IP_3 and Ca^{2+}. *Nature* **458**, 655-659.

Ramos-Franco, J., Bare, D., Caenepeel, S., Nani, A., Fill, M. and Mignery, G. (2000). Single-channel function of recombinant type 2 inositol 1,4,5-trisphosphate receptor. *Biophys. J.* **79**, 1388-1399.

Ringer, S. (1883). A further contribution regarding the influence of the different constituents of the blood on the contraction of the heart. *J. Physiol.* **4**, 29-42.

Rios, E. (2018). Calcium-induced release of calcium in muscle: 50 years of work and the emerging consensus. *J. Gen. Physiol.* **150**, 521-537.

Rizzuto, R., De Stefani, D., Raffaello, A. and Mammucari, C. (2012). Mitochondria as sensors and regulators of calcium signalling. *Nat. Rev. Mol. Cell Biol.* **13**, 566-578.

Rodriguez, E. A., Campbell, R. E., Lin, J. Y., Lin, M. Z., Miyawaki, A., Palmer, A. E., Shu, X., Zhang, J. and Tsien, R. Y. (2017). The growing and glowing toolbox of fluorescent and photoactive proteins. *Trends Biochem. Sci.* **42**, 111-129.

Rossi, A. M., Riley, A. M., Potter, B. V. L. and Taylor, C. W. (2010). Adenophostins: high-affinity agonists of IP_3 receptors. *Curr. Top. Membr.* **66**, 209-233.

Rossi, A. M., Riley, A. M., Tovey, S. C., Rahman, T., Dellis, O., Taylor, E. J. A., Veresov, V. G., Potter, B. V. L. and Taylor, C. W. (2009). Synthetic partial agonists reveal key steps in IP_3 receptor activation. *Nat. Chem. Biol.* **5**, 631-639.

Rossi, A. M. and Taylor, C. W. (2013). High-throughput fluorescence polarization assay of ligand binding to IP_3 receptors. *Cold Spring Harbor Protocols* **2013**, 938-946.

Rossi, A. M., Tovey, S. C., Rahman, T., Prole, D. L. and Taylor, C. W. (2012). Analysis of IP_3 receptors in and out of cells. *Biochim. Biophys. Acta* **1820**, 1214-1227.

Saleem, H., Tovey, S. C., Molinski, T. F. and Taylor, C. W. (2014). Interactions of antagonists with subtypes of inositol 1,4,5-trisphosphate (IP_3) receptor. *Br. J. Pharmacol.* **171**, 3298-3312.

Saleem, H., Tovey, S. C., Rahman, T., Riley, A. M., Potter, B. V. L. and Taylor, C. W. (2012). Stimulation of inositol 1,4,5-trisphosphate (IP_3) receptor subtypes by analogues of IP_3. *PLoS ONE* **8**, e54877.

Schug, Z. T. and Joseph, S. K. (2006). The role of the S4-S5 linker and C-terminal tail in inositol 1,4,5-trisphosphate receptor function. *J. Biol. Chem.* **281**, 24431-24440.

Schulz, I. (1990). Permeabilizing cells: some methods and application for the study of intracellular processes. *Methods Enzymol.* **192**, 280-300.

Seo, M.-D., Velamakanni, S., Ishiyama, N., Stathopulos, P. B., Rossi, A. M., Khan, S. A., Dale, P., Li, C., Ames, J. B., Ikura, M. et al. (2012). Structural and functional conservation of key domains in $InsP_3$ and ryanodine receptors. *Nature* **483**, 108-112.

Smith, I. F. and Parker, I. (2009). Imaging the quantal substructure of single IP_3R channel activity during Ca^{2+} puffs in intact mammalian cells. *Proc. Natl. Acad. Sci. USA* **106**, 6404-6409.

Smith, I. F., Wiltgen, S. M., Shuai, J. and Parker, I. (2009). Ca^{2+} puffs originate from preestablished stable clusters of inositol trisphosphate receptors. *Sci. Signal.* **2**, ra77.

Spät, A., Bradford, P. G., McKinney, J. S., Rubin, R. P. and Putney, J. W., Jr. (1986). A saturable receptor for ^{32}P-inositol-1,4,5-trisphosphate in hepatocytes and neutrophils. *Nature* **319**, 514-516.

Stehno-Bittel, L., Lückhoff, A. and Clapham, D. E. (1995). Calcium release from the nucleus by $InsP_3$ receptor channels. *Neuron* **14**, 163-167.

Streb, H., Irvine, R. F., Berridge, M. J. and Schulz, I. (1983). Release of Ca^{2+} from a nonmitochondrial intracellular store in pancreatic acinar cells by inositol-1,4,5-trisphosphate. *Nature* **306**, 67-69.

Südhof, T. C., Newton, C. L., Archer, B. T., Ushkaryov, Y. A. and Mignery, G. A. (1991). Structure of a novel $InsP_3$ receptor. *EMBO J.* **10**, 3199-3206.

Supattapone, S., Worley, P. F., Baraban, J. M. and Snyder, S. H. (1988). Solubilization, purification, and characterization of an inositol trisphosphate receptor. *J. Biol. Chem.* **263**, 1530-1534.

Sureshan, K. M., Riley, A. M., Thomas, M. P., Tovey, S. C., Taylor, C. W. and Potter, B. V. (2012). Contribution of phosphates and adenine to the potency of adenophostins at the IP_3 receptor: synthesis of all possible bisphosphates of adenophostin A. *J. Med. Chem.* **55**, 1706-1720.

Takahashi, M., Tanzawa, K. and Takahashi, S. (1994). Adenophostins, newly discovered metabolites of *Penicillium brevicompactum*, act as potent agonists of the inositol 1,4,5-trisphosphate receptor. *J. Biol. Chem.* **269**, 369-372.

Taylor, C. W., Prole, D. L. and Rahman, T. (2009). Ca^{2+} channels on the move. *Biochemistry* **48**, 12062-12080.

Taylor, C. W., Tovey, S. C., Rossi, A. M., Lopez Sanjurjo, C. I., Prole, D. L. and Rahman, T. (2014). Structural organization of signalling to and from IP_3 receptors. *Biochem. Soc. Trans.* **42**, 63-70.

Terry, L. E., Alzayady, K. J., Furati, E. and Yule, D. I. (2018). Inositol 1,4,5-trisphosphate receptor mutations associated with human disease. *Messenger* **6**, 29-44.

Thillaiappan, N. B., Chavda, A. P., Tovey, S. C., Prole, D. L. and Taylor, C. W. (2017). Ca^{2+} signals initiate at immobile IP_3 receptors adjacent to ER-plasma membrane junctions. *Nat. Commun.* **8**, 1505.

Thorn, K. (2016). A quick guide to light microscopy in cell biology. *Mol. Biol. Cell* **27**, 219-222.

Thurley, K., Tovey, S. C., Moenke, G., Prince, V. L., Meena, A., Thomas, A. P., Skupin, A., Taylor, C. W. and Falcke, M. (2014). Reliable encoding of stimulus intensities within random sequences of intracellular Ca^{2+} spikes. *Sci. Signal.* **7**, ra59.

Uchida, K., Miyauchi, H., Furuichi, T., Michikawa, T. and Mikoshiba, K. (2003). Critical regions for activation gating of the inositol 1,4,5-trisphosphate receptor. *J. Biol. Chem.* **278**, 16551-16560.

Vais, H., Foskett, J. K. and Mak, D. O. (2011). $InsP_3R$ channel gating altered by clustering? *Nature* **478**, E1-E2.

Van Petegem, F. (2014). Ryanodine receptors: allosteric ion channel giants. *J. Mol. Biol.* **427**, 31-53.

Wassler, M., Jonasson, I., Persson, R. and Fries, E. (1987). Differential permeabilization of membranes by saponin treatment of isolated rat hepatocytes. Release of secretory vesicles. *Biochem. J.* **247**, 407-415.

Watras, J., Bezprozvanny, I. and Ehrlich, B. E. (1991). Inositol 1,4,5-trisphosphate-gated channels in cerebellum: presence of multiple conductance states. *J. Neurosci.* **11**, 3239-3245.

Worley, P. F., Baraban, J. M., Supattapone, S., Wilson, V. S. and Snyder, S. H. (1987). Characterization of inositol trisphosphate receptor binding in brain. Regulation by pH and calcium. *J. Biol. Chem.* **262**, 12132-12136.

Xie, X., Xu, A. M., Leal-Ortiz, S., Cao, Y., Garner, C. C. and Melosh, N. A. (2013). Nanostraw-electroporation system for highly efficient intracellular delivery and transfection. *ACS Nano* **7**, 4351-4358.

Yamazaki, H., Chan, J., Ikura, M., Michikawa, T. and Mikoshiba, K. (2010). Tyr-167/Trp-168 in type1/3 inositol 1,4,5-trisphosphate receptor mediates functional coupling between ligand binding and channel opening. *J. Biol. Chem.* **285**, 36081-36091.

Yan, Z., Bai, X. C., Yan, C., Wu, J., Li, Z., Xie, T., Peng, W., Yin, C. C., Li, X., Scheres, S. H. et al. (2015). Structure of the rabbit ryanodine receptor RyR1 at near-atomic resolution. *Nature* **517**, 50-55.

Yen, M. and Lewis, R. S. (2018). Physiological CRAC channel activation and pore properties require STIM1 binding to all six Orai1 subunits. *J. Gen. Physiol.* **In press**.

Yoshikawa, F., Morita, M., Monkawa, T., Michikawa, T., Furuichi, T. and Mikoshiba, K. (1996). Mutational analysis of the ligand binding site of the inositol 1,4,5-trisphosphate receptor. *J. Biol. Chem.* **271**, 18277-18284.

Zalk, R., Clarke, O. B., Georges, A. D., Grassucci, R. A., Reiken, S., Mancia, F., Hendrickson, W. A., Frank, J. and Marks, A. R. (2015). Structure of a mammalian ryanodine receptor. *Nature* **517**, 44-49.

Zsolnay, V., Fill, M. and Gillespie, D. (2018). Sarcoplasmic reticulum Ca^{2+} release uses a cascading network of intra-SR and channel countercurrents. *Biophys. J.* **114**, 462-473.

Fig. 1: Ca^{2+} release by IP_3 and ryanodine receptors. (A) Many receptors in the plasma membrane (PM), including G-protein-coupled receptors (GPCRs) and receptor tyrosine kinases (RTKs), stimulate phospholipases C (PLC), causing hydrolysis of the PM lipid, phosphatidylinositol 4,5-bisphosphate, into diacylglycerol and IP_3. IP_3 binds to each of the four IP_3-binding sites of the tetrameric IP_3R to initiate conformational changes that lead to channel opening and release of Ca^{2+} from the ER. IP_3 is deactivated by phosphorylation to IP_4 or dephosphorylation to IP_2. RyRs are close relatives of IP_3Rs, but they are predominantly expressed in the sarcoplasmic reticulum of skeletal (RyR1) and cardiac (RyR2) muscle. Each RyR is activated when depolarization of the PM activates voltage-gated Ca^{2+} channels (Ca_v1). RyR1 are directly activated by conformational coupling to $Ca_V1.1$, whereas Ca^{2+} entering cardiac myocytes through $Ca_v1.2$ activates RyR2 through Ca^{2+}-induced Ca^{2+} release (CICR). Structures from Electron Microscopy Data Bank (IP_3R, EMD-5278 (Ludtke et al., 2011); RyR1, EMD-1275 (Ludtke et al., 2005)). (B) IP_3 binding is not alone sufficient to activate IP_3Rs. IP_3 binding primes IP_3Rs to bind Ca^{2+} and that leads to channel opening. All four IP_3-binding sites must be occupied for the pore to open, but it is not yet known how many Ca^{2+}-binding sites must be occupied (we show four for simplicity). (C) Dual regulation of IP_3Rs by IP_3 and Ca^{2+} allows them to propagate regenerative Ca^{2+} signals by CICR. Local CICR activity within a small cluster of IP_3Rs generates a Ca^{2+} puff. (D) The vicinal 4,5-bisphosphate moiety of IP_3 is essential for activity, whereas the 1-phosphate enhances affinity. (E) IP_3 is recognised by the IP_3-binding core (IBC) of IP_3R. The essential 4- and 5-phosphates of IP_3 interact with opposing sides of the clam-like IBC to cause clam closure. The loop of the suppressor domain (SD) interacts with IBC-β of a neighbouring subunit (Seo et al., 2012). A-C modified from Taylor et al. (2014), and D reproduced from Seo et al. (2012).

Fig. 2: Measuring IP_3 binding to IP_3Rs. (A) Binding assays allow determination of the equilibrium dissociation constant (K_D) (**Box 2**). Non-equilibrium measurements allow rate constants (k_{+1} and k_{-1}) to be determined. (B) Commonly, radioactive IP_3 (typically ^3H-IP_3) is equilibrated with IP_3R before rapidly separating (usually by centrifugation) bound and free ligands to determine the amount of ^3H-IP_3 bound to its receptor. (C) By immobilizing IP_3R on the surface of a bead that detects only immediately adjacent (i.e. bound) ^3H-IP_3, scintillation proximity assays (SPA) report bound ^3H-IP_3 without separating bound from free ligand (Patel et al., 1996). (D) A variety of methods, including surface-plasmon resonance (SPR), fluorescence correlation spectroscopy (FCS) and fluorescence polarization (FP) rely on detecting the large increase in apparent size of IP_3 as it binds to the IP_3R (or a fragment of it). With FP, for example (illustrated), a fluorescent analogue of IP_3 rotates rapidly when free, but less so when it has bound to a soluble IP_3R fragment. The difference can be measured, without separating bound and free ligands, by recording the extent to which plane-polarized light remains polarized (Ding et al., 2010). (E) Isothermal titration calorimetry (ITC) measures the very small amounts of heat released or absorbed (ΔH) as IP_3 binds to purified IP_3R by comparison with a reference cell (de Azevedo and Dias, 2008).

Fig. 3: Towards understanding how IP_3 and Ca^{2+} open IP_3Rs. (A) Single IP_3R1 subunit showing key domains: the N-terminal suppressor domain (SD); the β and α domains of the IP_3-binding core (IBC); the intervening lateral domain (ILD), which lies between ARM3 and the first trans-membrane domain (TMD1); TMD6, which lines the pore and is occluded by hydrophobic residues towards its cytosolic end in the closed state; the helical linker domain (LNK); and the C-terminal α-helical domain (CTD), which is unique to IP_3Rs. The structure was published in Fan et al. (2015) (Protein Data Base, PDB 3JAV). (B) Simplified scheme, derived from structures of IP_3R1 (Fan et al., 2015) and IP_3R3 (Paknejad and Hite, 2018) shows that the only contact between the cytosolic and pore region occurs at the nexus between ARM3 with its C-terminal ILD domain and the C-terminal extension of TMD6 (LNK). These contacts form an interleaved structure, with residues from LNK and the base of ARM3 cooperating to form a Ca^{2+}-binding site. Binding sites for IP_3 (IBC-α and IBC-β) and Ca^{2+} are formed by residues contributed from different domains, allowing rigid-body movements of domains to reconfigure the sites. The first Ca^{2+}-binding site assembles from residues provided by ARM1 and the α-helical linker between ARM1 and ARM2. The second Ca^{2+}-binding site is structurally conserved in RyR, and assembled by residues from ARM3 and LNK domains. This second site may mediate the IP_3-regulated binding of Ca^{2+} that precedes channel opening (see text for details) (Paknejad and Hite, 2018). Opening of the pore requires movement of occluding hydrophobic residues that lie close to the cytosolic end of TMD6; Ca^{2+} can then pass rapidly form the ER lumen to the cytosol.

Box 1: IP_3Rs and RyRs are not the only intracellular Ca^{2+} channels

IP_3Rs and RyRs are the major intracellular Ca^{2+}-release channels in most cells and the major links between extracellular stimuli and Ca^{2+} release from the ER or sarcoplasmic reticulum (SR) (**Fig. 1A**), but they are not the only intracellular Ca^{2+} channels (Taylor et al., 2009). Polycystin-2 (also known as TRPP2), a member of the transient receptor potential (TRP) superfamily, is also expressed in the ER and is activated by Ca^{2+} (Koulen et al., 2002). A variety of Ca^{2+}-permeable channels are expressed in lysosomes, including those regulated by luminal pH and ATP (P2X purinoceptor 4, P2X4) (Huang et al., 2014), cytosolic nicotinic acid adenine dinucleotide phosphate (NAADP; two pore channel 2, TPC2) (Morgan and Galione, 2013), and the lysosomal membrane lipid, phosphatidylinositol 3,5-bisphosphate (transient receptor potential mucolipin 1 channel, TRPML1) (Cao et al., 2017). The mitochondrial uniporters (MCU) comprise another important family of intracellular Ca^{2+} channels (Oxenoid et al., 2016; Patron et al., 2013). Opening of MCU is triggered by large local increases in $[Ca^{2+}]_c$, causing Ca^{2+} to flow rapidly from the cytosol across the inner mitochondrial membrane and into the mitochondrial matrix, where Ca^{2+} regulates many activities (Rizzuto et al., 2012). A recurrent theme in Ca^{2+} signalling is the importance of interactions between Ca^{2+} channels in different membranes: store-operated Ca^{2+} entry is activated after loss of Ca^{2+} from the ER through IP_3Rs; mitochondrial Ca^{2+} uptake is driven by local Ca^{2+} release through IP_3Rs and RyRs (Csordas et al., 2018); NAADP-evoked Ca^{2+} release from lysosomes is amplified by CICR through closely apposed IP_3Rs or RyRs (Morgan and Galione, 2013); and Ca^{2+} puffs and sparks are ignited by CICR triggering Ca^{2+} release within clusters of IP_3Rs or RyRs (**Fig. 1C**) (Cheng and Lederer, 2008; Rios, 2018; Thillaiappan et al., 2017).

Box 2: Analysis of IP_3 binding

Analyses of IP_3 binding allow affinities of IP_3 or competing ligands to be determined (as equilibrium dissociation constants, K_D, the concentration of IP_3 at which 50% of binding sites are occupied) (**Fig. 2**). These analyses determine the relationship between the concentration of a ligand and the amount bound to IP_3Rs. Radioligand binding, using ^{3}H-IP_3, is the most commonly used approach. Most methods used to determine specific binding of ^{3}H-IP_3 to IP_3Rs require rapid separation of bound and free ^{3}H-IP_3, such that the equilibrium between free ^{3}H-IP_3, competing ligands and the IP_3R is not perturbed by the separation procedure (filtration or centrifugation) (**Fig. 2A,B**). Measuring specific binding with different concentrations of ^{3}H-IP_3 allows the K_D for ^{3}H-IP_3 to be determined, whereas measuring specific binding of ^{3}H-IP_3 in the presence of different concentrations of a competing ligand allow the K_D of that ligand to be determined (Cheng and Prusoff, 1973). Advantages of these ^{3}H-IP_3 binding assays are their simplicity and applicability to IP_3Rs within membranes, after detergent-solubilization or as IP_3-binding fragments (Rossi et al., 2009). Scintillation proximity assays (SPA) avoid the need for separation steps because the SPA beads are impregnated with a scintillant, such that when IP_3Rs are immobilized on the surface of the bead, only ^{3}H-IP_3 bound to an IP_3R is detected (**Fig. 2C**) (Patel et al., 1996). More specialized methods allow analysis of ligand binding to IP_3Rs without using radioligands. These methods include fluorescence polarization (FP), which uses a fluorescent analogue of IP_3 to report the size of the molecule to which the fluorophore is attached. When free, the fluorescent IP_3 is small and tumbles rapidly in solution, but when bound to a large IP_3R fragment it tumbles more slowly. These changes can be detected using plane-polarized light (**Fig. 2D**) (Ding et al., 2010; Rossi and Taylor, 2013). Isothermal titration calorimetry (ITC), which measures heat exchange during IP_3 binding, is another means of measuring ligand binding to IP_3Rs without using ^{3}H-IP_3 (**Fig. 2E**) (de Azevedo and Dias, 2008). Limitations of both FP and ITC include the need for both specialised equipment and large amounts of purified protein.

Box 3: Nuclear patch-clamp recordings can be applied to IP_3Rs

Patch-clamp recording allows the opening and closing of single ion channels to be recorded with exquisite sensitivity (Neher, 1992). Usually these recordings are made at the plasma membrane (PM), but that is not applicable to single-channel recordings from IP_3Rs, most of which are expressed in ER. However, the outer nuclear membrane (ONM) is continuous with the ER membrane, and IP_3Rs are expressed in the ONM. A glass microelectrode applied to the ONM of an isolated nucleus allows single-channel recording from IP_3Rs trapped within. By excising the patch from the intact nucleus to provide an excised patch, it is possible to make recordings with the IP_3-binding site of the IP_3R exposed to either the interior of the patch-pipette patch or (with greater difficulty) to the bath solution (Mak et al., 2007). The latter allows rapid application of IP_3 or Ca^{2+} to the cytosolic surface. K^+ or Cs^+ are commonly used as charge-carriers for patch-clamp recording because they provide large currents and they, unlike Ca^{2+}, do not regulate IP_3R gating. These patch-clamp methods allow the ion selectivity and conductance of IP_3Rs to be determined. By examining the sequence of channel openings and closing, gating schemes can be developed that seek to explain how regulators of IP_3Rs (like IP_3 and Ca^{2+}) move the channel through different closed states to its open state (Mak and Foskett, 2014; Rahman et al., 2009). Image reproduced, with permission, from Rossi et al. (2012).

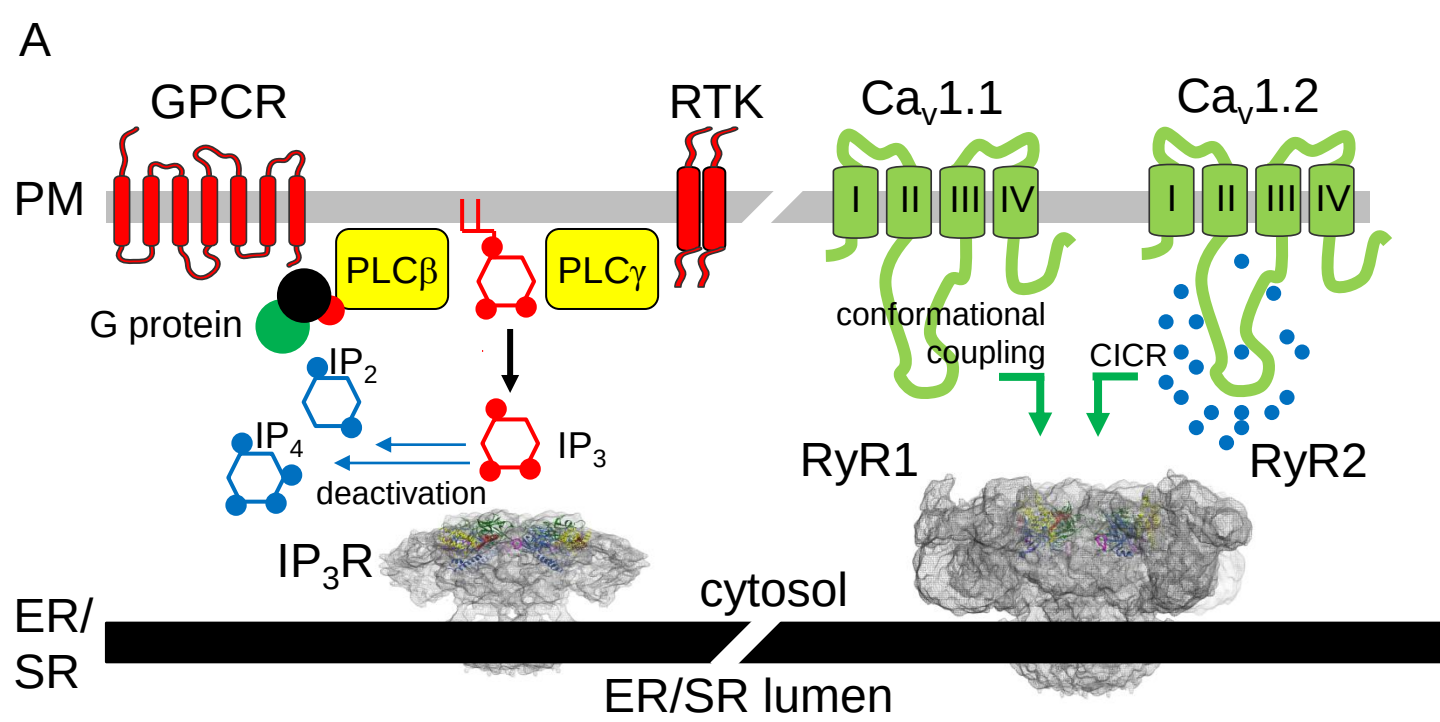
A
GPCR
RTK
PM
PLCβ
PLCγ
G protein
IP2
IP4
IP3
deactivation
IP3R
ER/
SR
cytosol
ER/SR lumen
CaV1.1
CaV1.2
I
II
III
IV
conformational
coupling
CICR
RyR1
RyR2

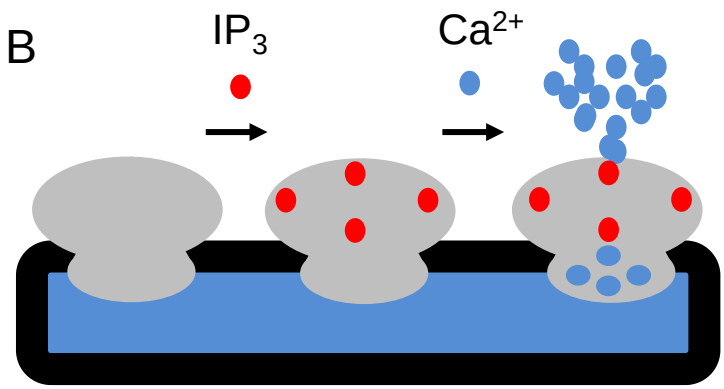
B
IP3
Ca2+

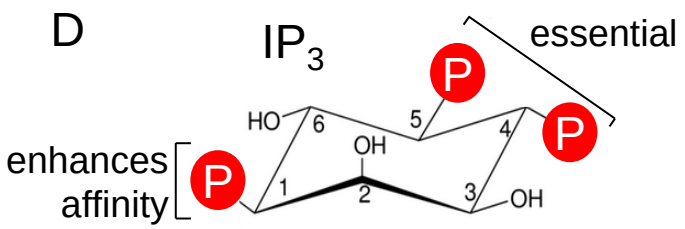
D
IP3
essential
enhances
affinity
P
HO
OH
OH
1
2
3
4
5
6

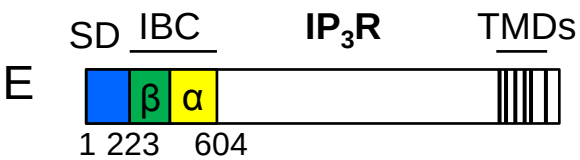
E
SD
IBC
IP3R
TMDs
β
α
1
223
604

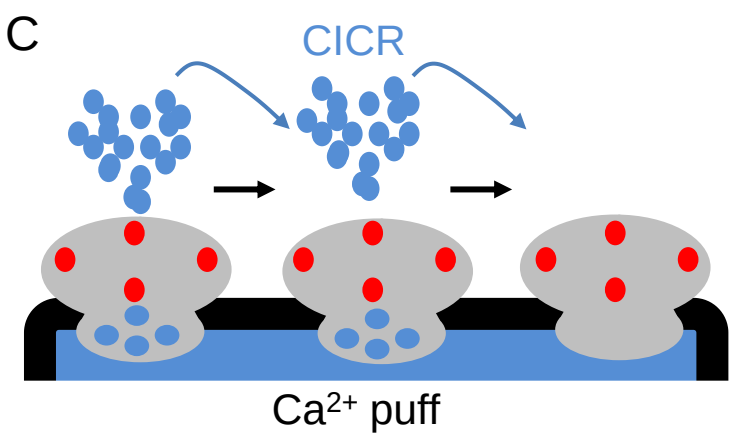
C
CICR
Ca2+ puff

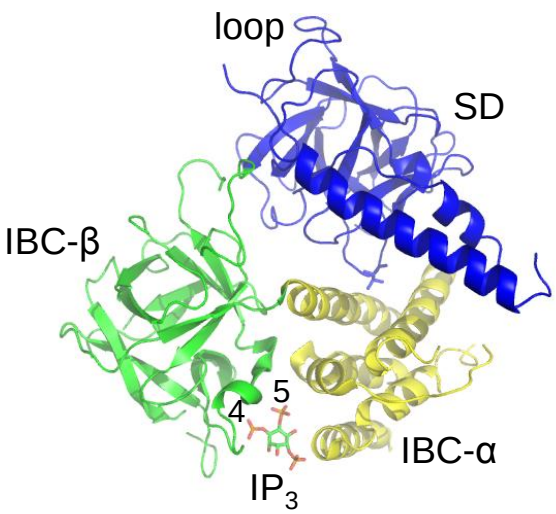
loop
SD
IBC-β
IBC-α
4
5
IP3

Figure 1

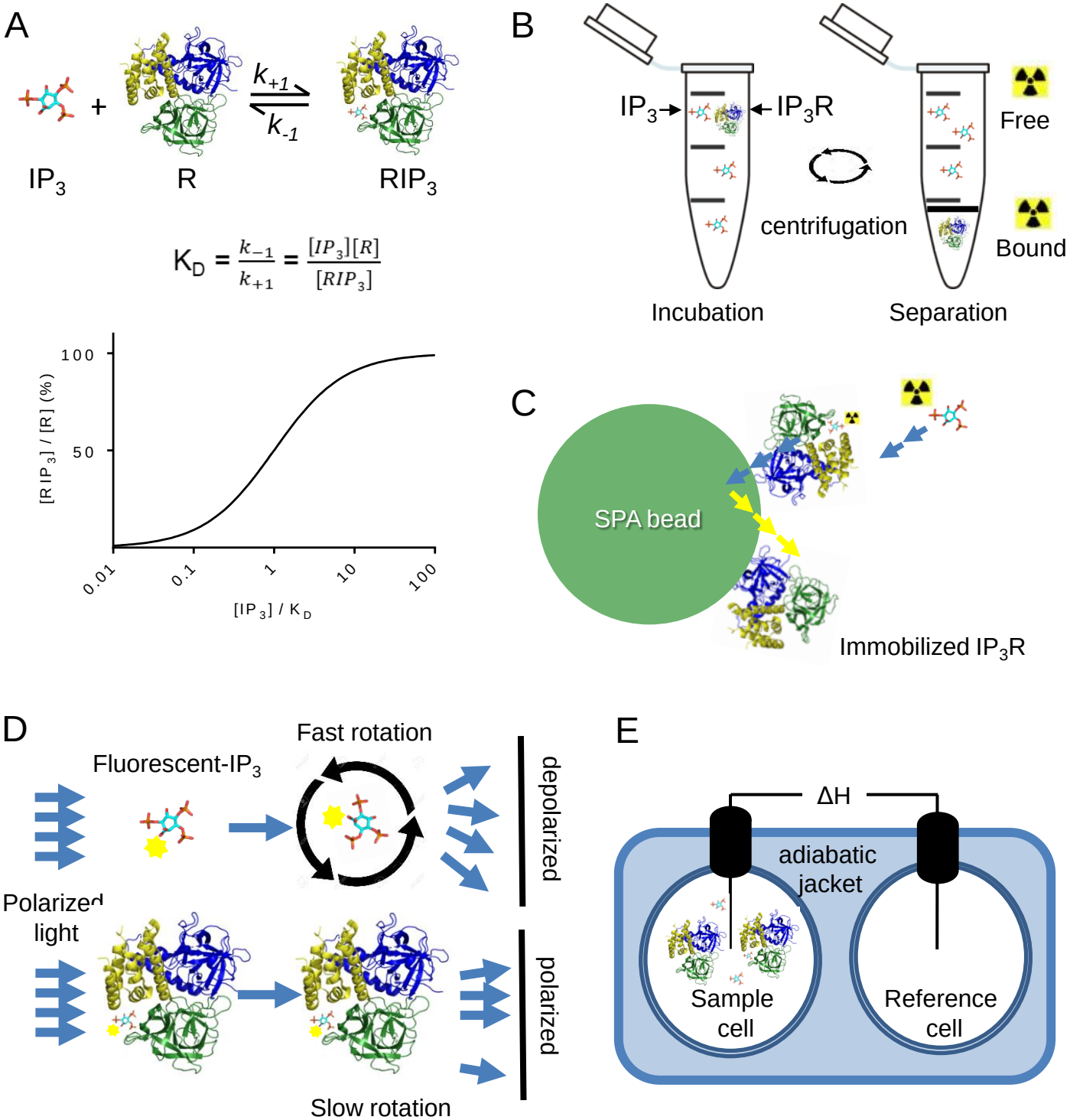
A
IP3
R
RIP3
k+1
k-1
KD = k−1 / k+1 = [IP3][R] / [RIP3]
100
50
[R IP3] / [R] (%)
0.01
0.1
1
10
100
[IP3] / KD
B
IP3
IP3R
centrifugation
Free
Bound
Incubation
Separation
C
SPA bead
Immobilized IP3R
D
Fast rotation
Fluorescent-IP3
Polarized light
depolarized
polarized
Slow rotation
E
ΔH
adiabatic jacket
Sample cell
Reference cell

Figure 2

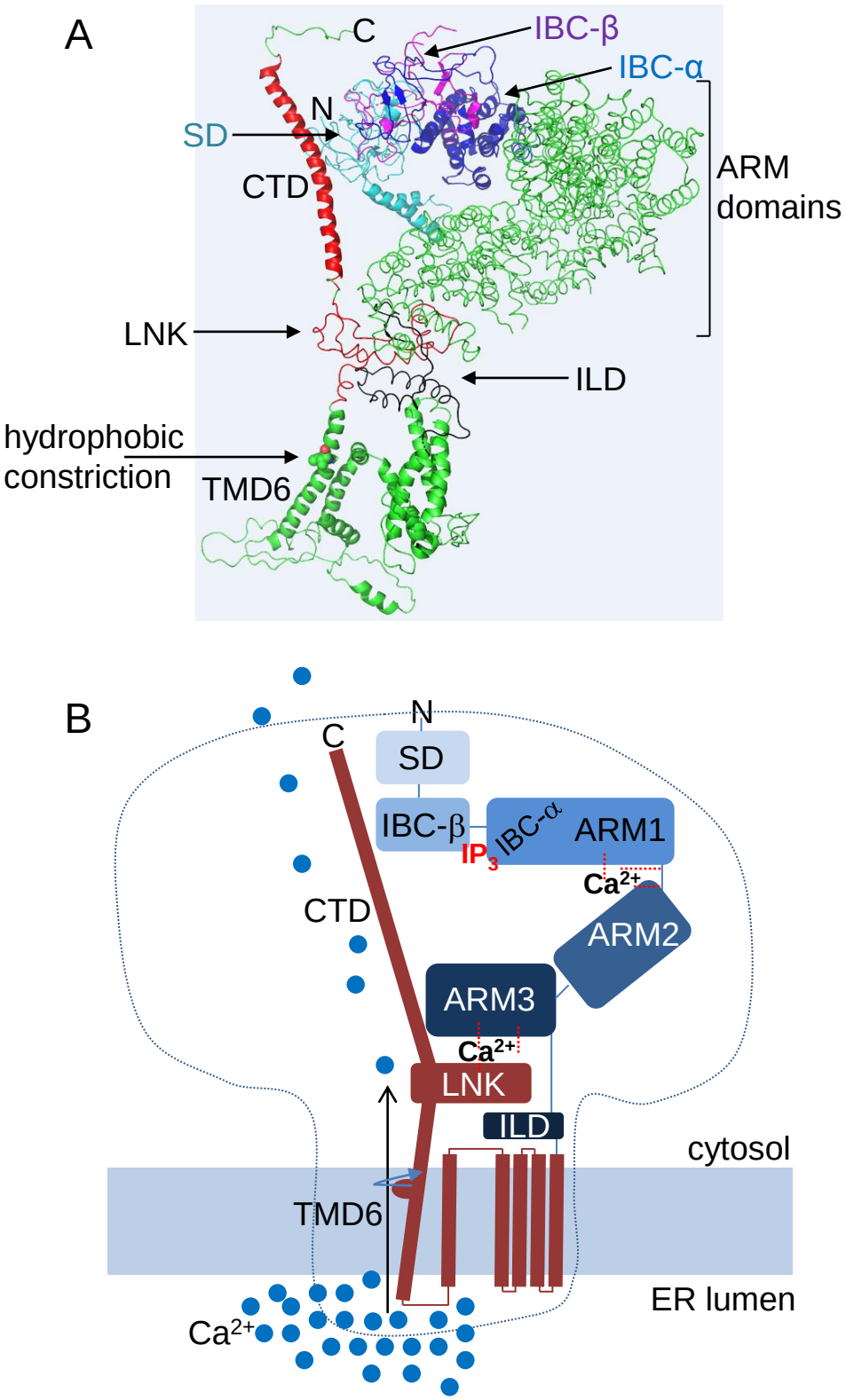
A
C
IBC-β
IBC-α
N
SD
CTD
ARM
domains
LNK
ILD
hydrophobic
constriction
TMD6
B
N
C
SD
IBC-β
IBC-α
ARM1
IP3
Ca2+
CTD
ARM2
ARM3
Ca2+
LNK
ILD
cytosol
TMD6
ER lumen
Ca2+

Figure 3

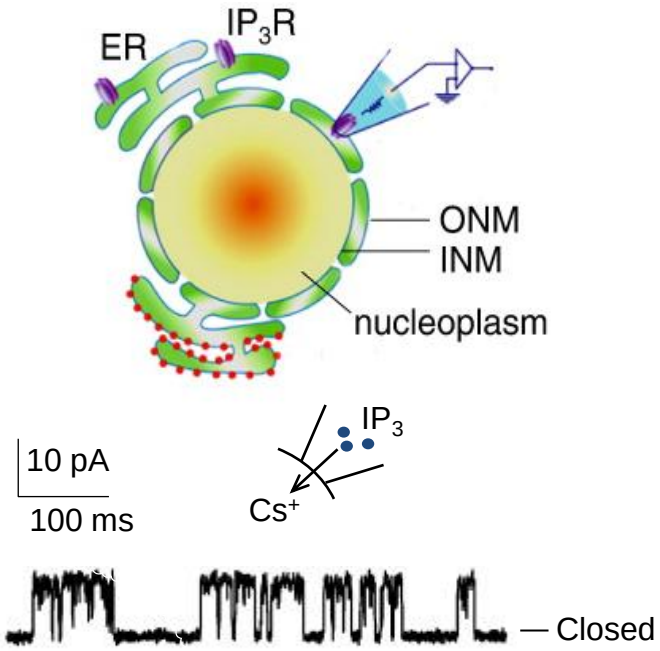

For Box 3